

# Orientation control of high- $\chi$ triblock copolymer for sub-10 nm patterning using fluorine-containing polymeric additives

Jiajing Li  
Chun Zhou  
Xuanxuan Chen  
Paulina A. Rincon Delgadillo  
Paul F. Nealey

# Orientation control of high- $\chi$ triblock copolymer for sub-10 nm patterning using fluorine-containing polymeric additives

Jiajing Li,<sup>a</sup> Chun Zhou,<sup>a</sup> Xuanxuan Chen,<sup>a</sup> Paulina A. Rincon Delgadillo,<sup>b</sup> and Paul F. Nealey<sup>a,c,\*</sup>

<sup>a</sup>University of Chicago, Pritzker School of Molecular Engineering, Chicago, Illinois, United States

<sup>b</sup>IMEC, Leuven, Belgium

<sup>c</sup>Argonne National Laboratory, Material Science Division, Lemont, Illinois, United States

**Abstract.** Directed self-assembly (DSA) of block copolymers (BCPs) is one of the most promising techniques to tackle the ever-increasing demand for sublithographic features in semiconductor industries. BCPs with high Flory–Huggins parameter ( $\chi$ ) are of particular interest due to their ability to self-assemble at the length scale of sub-10 nm. However, such high- $\chi$  BCPs typically have imbalanced surface energies between respective blocks, making it a challenge to achieve desired perpendicular orientation. To address this challenge, we mixed a fluorine-containing polymeric additive with poly(2-vinylpyridine)-*block*-polystyrene-*block*-poly(2-vinylpyridine) (P2VP-*b*-PS-*b*-P2VP) and successfully controlled the orientation of the high- $\chi$  triblock copolymer. The additive selectively mixes with P2VP block through hydrogen bonding and can reduce the dissimilarity of surface energies between PS and P2VP blocks. After optimizing additive dose and annealing conditions, desired perpendicular orientation formed upon simple thermal annealing. We further demonstrated DSA of this material system with five times density multiplication and a half-pitch as small as 8.5 nm. This material system is also amenable to sequential infiltration synthesis treatment to selectively grow metal oxide in P2VP domains, which can facilitate the subsequent pattern transfer. We believe that this integration-friendly DSA platform using simple thermal annealing holds the great potential for sub-10 nm nanopatterning applications. © 2019 Society of Photo-Optical Instrumentation Engineers (SPIE) [DOI: 10.1117/1.JMM.18.3.035501]

Keywords: directed self-assembly; block copolymer; lithography; sub-10 nm; sequential infiltration synthesis.

Paper 19039 received May 17, 2019; accepted for publication Jul. 3, 2019; published online Jul. 25, 2019.

## 1 Introduction

The linear dimensions of transistors have been reduced by half every three years during the past five decades, which was mainly accomplished by reducing the wavelength of light used in lithography. The current state-of-the-art immersion photolithography tools using deep ultraviolet light with wavelength of 193 nm can reach 40-nm resolution limit with a single exposure. However, when the wavelength goes further down to the extreme ultraviolet at 13.5 nm, considerable challenges are faced such as the tool cost, uptime, and stochastic variations. As an alternative technique for ultra-high resolution patterning, directed self-assembly (DSA) has attracted great academic and industrial interest since it was first introduced over a decade ago.<sup>1</sup>

DSA is a patterning technique that orders the self-assembling block copolymers (BCPs) using a chemical or topographical template. The assembly of BCPs is well guided by the template, and the resulted structures resemble critical features in integrated circuits such as line/space and contact holes. DSA is especially attractive due to its ability to multiply the density of lithographical features of the template, denoted as density multiplication, which can extend optical lithography far beyond its current limits.<sup>2</sup> Polystyrene-*block*-poly(methyl methacrylate) (PS-*b*-PMMA) is the most widely studied BCP for DSA applications because of the similar surface energies of PS and PMMA blocks, which enables desired perpendicular orientation by thermal annealing with

a free surface. DSA of PS-*b*-PMMA with 14-nm half-pitch line/space pattern has been implemented on 300-mm wafer processing line at IMEC with relatively low defect density, approaching that required for high-volume manufacturing.<sup>3</sup> However, PS-*b*-PMMA has a resolution limit of 11 nm due to its low Flory–Huggins interaction parameter ( $\chi$ ), which prevents microphase separation and pattern transfer at smaller pitch.<sup>4</sup> As a result, it is imperative to explore more BCPs with higher  $\chi$  to achieve the desired sub-10 nm feature size.

One promising high- $\chi$  BCP is poly(2-vinylpyridine)-*block*-polystyrene-*block*-poly(2-vinylpyridine) (P2VP-*b*-PS-*b*-P2VP) with  $\chi$  equal to 0.10 at 200°C compared with 0.037 for that of PS-*b*-PMMA.<sup>5</sup> Though higher  $\chi$  enables P2VP-*b*-PS-*b*-P2VP (VSV) to microphase separate into lamellar structures at sub-10 nm feature size, forming perpendicularly oriented BCP domains remains a challenge due to imbalanced surface energies of PS and P2VP blocks.<sup>6</sup> The surface tension of PS is 40.7 mN m<sup>-1</sup> and that of P2VP is 49.4 mN m<sup>-1</sup>,<sup>7</sup> resulting in undesired parallel orientation upon annealing. Several approaches have been developed to circumvent the problem of dissimilar surface energies, including solvent vapor annealing,<sup>8</sup> vapor-phase deposited top coat,<sup>9</sup> and embedded neutral layer.<sup>10</sup> Despite the successful orientation control these approaches have achieved, challenges still remain to meet all the requirements for large-scale manufacturing. For example, there is no solvent annealing tool currently available for manufacturing, and top

\*Address all correspondence to Paul F. Nealey, E-mail: [nealey@uchicago.edu](mailto:nealey@uchicago.edu)

coat approaches require additional processing steps, which lead to increased complexity and costs. The segregated neutral layer topcoat also brings challenges for pattern transfer by dry etching.

Our strategy to control the orientation of VSV is to use a fluorine-containing polymeric additive poly(hexafluoroalcohol styrene) (PHFAS), which enables perpendicular orientation of VSV by simple thermal annealing. The same polymeric additive has been shown to effectively tune the surface energies of other BCPs.<sup>11</sup> PHFAS has lower surface energy than both PS and P2VP blocks and can selectively interact with P2VP via hydrogen bonding to lower the apparent surface energy of P2VP block. By carefully adjusting the amount of PHFAS in the system, the surface energies of PS and P2VP blocks can be balanced and desired perpendicular orientation can form upon thermal annealing. After optimizing PHFAS dose and annealing conditions, we further demonstrate DSA of VSV/PHFAS with density multiplication on chemical patterns. We also investigate the pattern transfer potential of this material system assisted by sequential infiltration synthesis (SIS). Finally, we discuss the impact of molecular weight of PHFAS on orientation control and offer a simple yet effective way to predict the molecular weight of PHFAS needed for a given VSV.

## 2 Experiment

### 2.1 Materials

VSV with three different molecular weights ( $M_n = 26, 33,$  and  $47 \text{ kg} \cdot \text{mol}^{-1}$ ) were purchased from Polymer Source, Inc. PHFAS additives with two molecular weights ( $M_n = 4.4 \text{ kg} \cdot \text{mol}^{-1}, M_w = 5.9 \text{ kg} \cdot \text{mol}^{-1}; M_n = 6.7 \text{ kg} \cdot \text{mol}^{-1}, M_w = 9.5 \text{ kg} \cdot \text{mol}^{-1}$ ) were synthesized via free-radical polymerization, as described elsewhere.<sup>11</sup> Hydroxyl-terminated polystyrene-*random*-poly(2-vinylpyridine) (PS-*r*-P2VP-OH)

was synthesized in our group, as previously reported.<sup>12</sup> Silicon (100) wafers were purchased from WRS Materials, LLC (San Jose, California, United States). All solvents were purchased from Aldrich and used as received.

### 2.2 Self-Assembly of VSV with PHFAS Additive

A solution of 1.5 wt% PS-*r*-P2VP-OH in dimethylformamide (DMF) was spin-coated on clean silicon wafers followed by annealing at 200°C for 10 min under a nitrogen atmosphere. The brush was grafted on the surface via reaction between hydroxyl group at the chain end and the silicon oxide surface. Ungrafted polymer brush was removed by sonication in DMF and the substrates were dried with nitrogen. The thickness of grafted brush was  $\sim 8 \text{ nm}$ . Brush modified wafers were then coated with 1 wt% VSV/PHFAS solution in DMF and annealed under a nitrogen atmosphere. The thickness of VSV/PHFAS film after annealing was  $\sim 20 \text{ nm}$ .

### 2.3 Directed Self-Assembly of VSV with PHFAS Additive

The DSA process was adapted from previously reported process.<sup>13</sup> Briefly, silicon wafers were spin-coated with cross-linkable polystyrene solution and annealed at 250°C for 5 min under a nitrogen atmosphere to drive the cross-linking reaction. Chemical patterns were prepared using electron-beam (E-beam) lithography followed by exposure to oxygen plasma, which trimmed the cross-linked polystyrene (xPS) guiding stipes to the desired width. After oxygen plasma, the excess resist was removed by repeated sonication in *N*-methyl-2-pyrrolidone and chlorobenzene. Alternatively, silicon wafers with xPS guiding stripes were also received from IMEC prepared by a previously reported approach.<sup>14</sup> PS-*r*-P2VP-OH brush was then grafted onto the

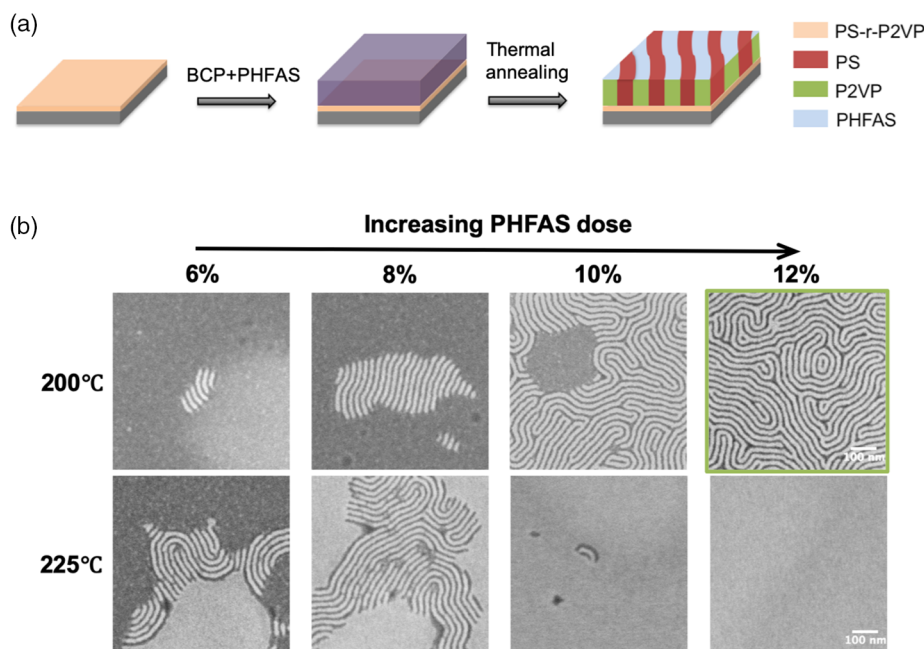


**Fig. 1** (a) Process flow for self-assembly of VSV with PHFAS additive. (b) SEM images of VSV with various doses of PHFAS upon thermal annealing on neutral substrates. Brighter domain is P2VP and darker domain is PS. Full perpendicular orientation forms with 12% PHFAS at 200°C.  $L_0$  is 23.0 nm as measured from FFT analysis.

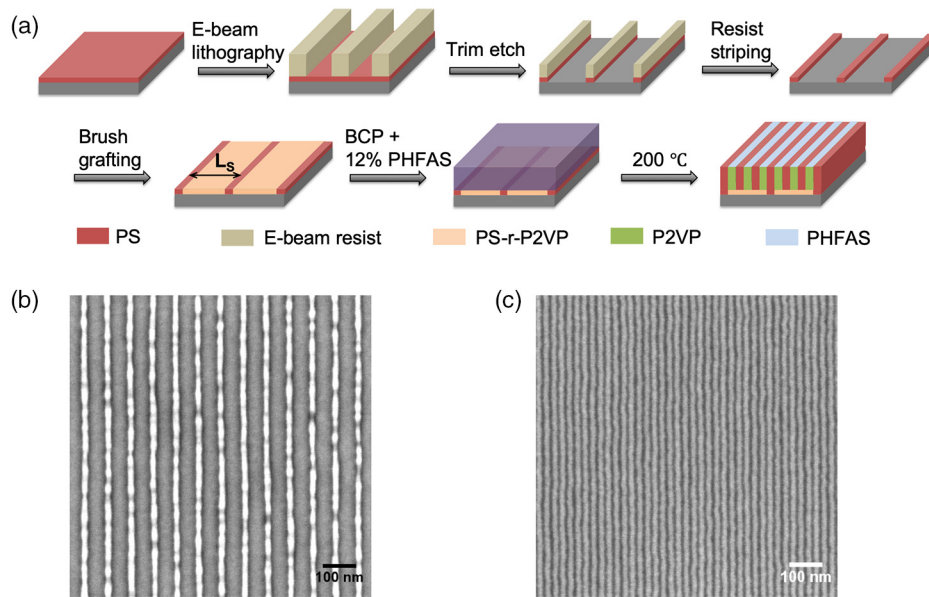


**Fig. 2** (a) Process flow for chemoepitaxy DSA of VSV with PHFAS additive, (b) SEM image of the template after trim etch, and (c) DSA pattern with 23.0 nm full pitch after assembly.

wafers and VSV film with optimized PHFAS dose was annealed under a nitrogen atmosphere.

### 3 Results and Discussion

#### 3.1 Orientation Control of VSV with PHFAS Additive

To achieve desired perpendicular orientation, both interfacial energies between substrate and BCP as well as surface energies between BCP and nitrogen atmosphere need to be balanced. Interfacial energies can be readily tuned by employing random copolymer brush with optimized PS content, which is nonpreferential to respective blocks.<sup>12</sup> For VSV, however, surface energies are not balanced since surface energy of PS is lower than that of P2VP. To reduce this dissimilarity, we introduce PHFAS as a surface energy balancer to lower the apparent surface energy of P2VP.

We first investigate two possible factors that might affect the orientation control of VSV: PHFAS dose and annealing temperatures. We start with a relatively large VSV ( $47 \text{ kg} \cdot \text{mol}^{-1}$ ) to optimize these factors following the schematic in Fig. 1(a). The substrate is modified with PS-*r*-P2VP-OH brush containing 48% PS, which has been identified nonpreferential to VSV.<sup>12</sup> VSV solutions with various doses of PHFAS ( $M_w = 9.5 \text{ kg} \cdot \text{mol}^{-1}$ ) are spin-coated on brush modified substrates and annealed under nitrogen atmosphere at different temperatures.

When PHFAS dose is low (below 6 wt%), parallel lamellae are the predominant structures due to imbalanced surface energies [Fig. 1(b)]. PS block is more favored by the top surface than P2VP block due to its lower surface energy. As PHFAS dose increases, perpendicular orientation begins to form as a result of more balanced surface energies. When PHFAS dose reaches 12 wt% (with respect to VSV), full perpendicular orientation can be observed at 200°C. PHFAS is expected to stay in the P2VP block via the hydrogen bonding and is likely to aggregate on top of the P2VP block during annealing because of its lower surface energy. Periodicity ( $L_0$ ) of the self-assembled pattern is 23.0 nm as

measured by fast Fourier transform (FFT) analysis of the top-down scanning electron microscope (SEM) images. It is worth noting that  $L_0$  increases by  $\sim 7.5\%$  compared with that from solvent annealing,<sup>15</sup> which can be attributed to two possible reasons. It is likely that the effective  $\chi$  of VSV increases with the presence of PHFAS,<sup>16</sup> which can potentially lead to larger  $L_0$  and lower line edge roughness. In this case, PHFAS is most likely only distributed in the P2VP block as we hypothesized. If PHFAS is equally distributed in both blocks,  $\chi$  should decrease rather than increase. Alternatively, it is also possible that the presence of PHFAS can affect the chain conformations of P2VP block and thus increase  $L_0$ .

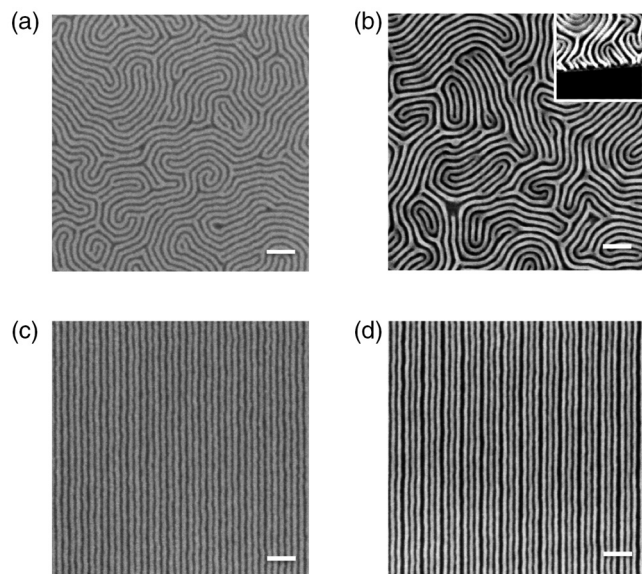


**Fig. 3** SEM images of assembled VSV (a, c) after SIS and (b, d) after oxygen plasma on neutral substrates and on chemical patterns. Scale bars represent 100 nm.

### 3.2 Directed Self-Assembly of VSV with PHFAS Additive

The self-assembly of lamellae-forming BCPs can be directed using chemically contrast patterns comprising of guiding stripes of cross-linked homopolymer mat and interspatial random copolymer brush,<sup>17</sup> which is usually denoted as chemoepitaxy DSA. The key to chemoepitaxy DSA is the ability of BCPs to recognize the chemical patterns and align along the guiding stripes based on the wetting preference. It is crucial that VSV still preserves this ability when mixed with PHFAS.

The chemoepitaxy DSA of VSV/PHFAS with three times density multiplication is demonstrated following the schematic shown in Fig. 2(a). The substrate is coated with xPS followed by E-beam lithography. After removing xPS in the exposed areas and trim etching the xPS guiding stripes underneath E-beam resist lines with oxygen plasma, the

E-beam resist is stripped and the exposed areas between xPS guiding lines are subsequently backfilled with the same neutral PS-*r*-P2VP-OH brush used in the orientation control. VSV (47k) with 12% PHFAS (9.5k) is spin-coated on chemical patterns and annealed at 200°C. Successful DSA with 23-nm full pitch [Fig. 2(c)] is demonstrated on a template with the initial pitch  $L_s = 69$  nm [Fig. 2(b)]. This confirms that the presence of PHFAS does not impair the ability of VSV to recognize the chemical contrast of the chemical patterns and thus, the standard chemoepitaxy DSA scheme is still valid.

### 3.3 Mask Conversion of BCP Pattern with SIS

To implement the DSA line/space patterns for advanced patterning applications, the patterns need to be transferred from the BCP films to the underlying substrates, which desires high etching contrast between different blocks of the BCP.

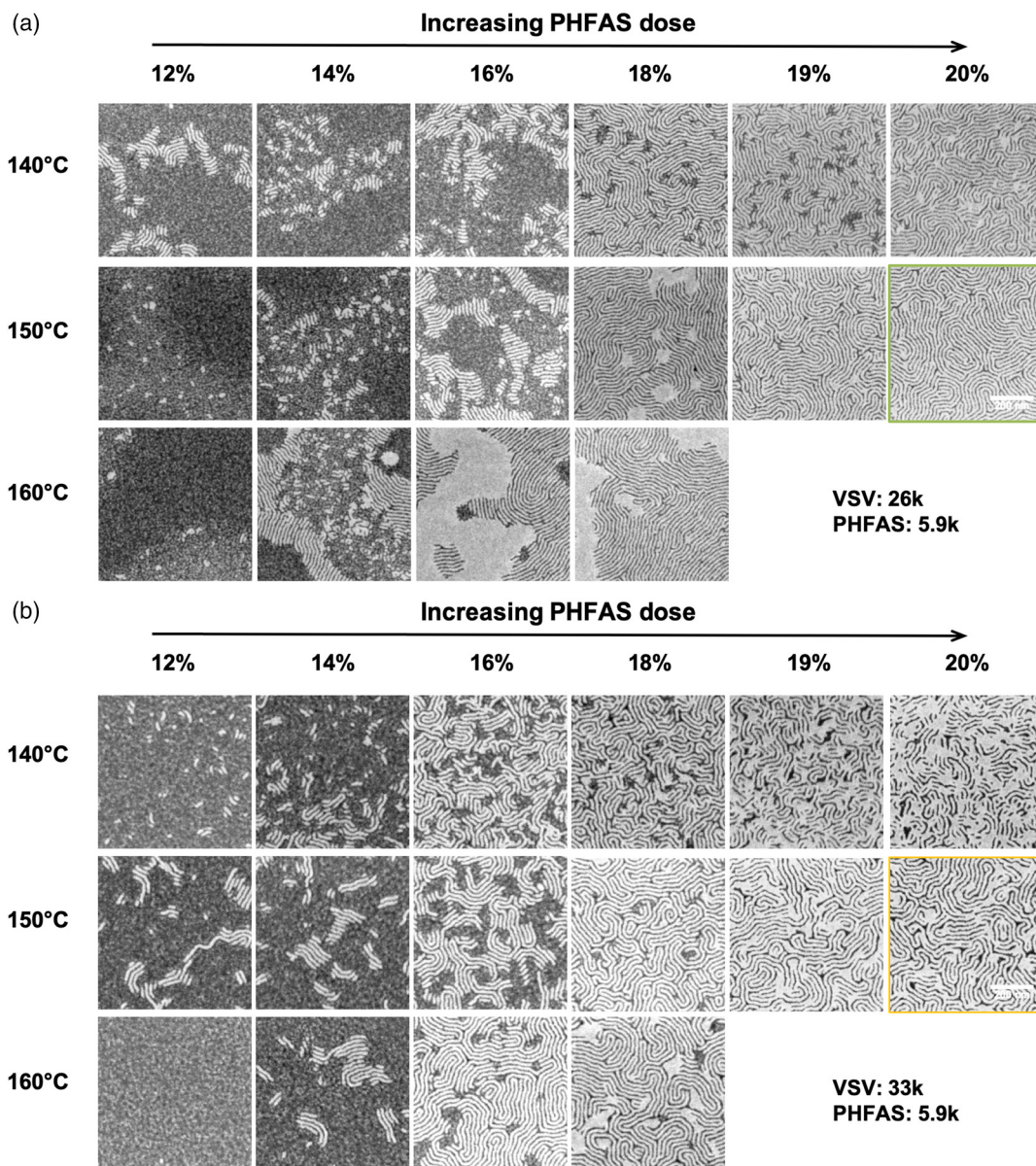


**Fig. 4** SEM images of 26k VSV and 33k VSV with various doses of 5.9k PHFAS upon thermal annealing on neutral substrates. (a) For 26k VSV, full perpendicular orientation forms with 20% PHFAS at 150°C. (b) For 33k VSV, no full perpendicular orientation can be observed. Scale bars represent 200 nm.

One effective way to increase the etching contrast of VSV is SIS, where metal oxide such as alumina selectively infiltrates the P2VP block, whereas PS block is relatively unaffected. VSV is then removed by oxygen plasma, leaving the alumina lines mimicking the original patterns of P2VP blocks, which afterward could be used as effective etching masks.<sup>18</sup> The alumina mask is more resistant to a variety of etching chemistries compared with the original soft matter films and thus could facilitate the direct pattern transfer to the underlying substrates without the need of an additional hard mask layer.<sup>8,9</sup> Our group has previously demonstrated pattern transfer of VSV to silicon substrates with 8-nm half-pitch using this technique.<sup>8</sup>

As PHFAS is also expected to form hydrogen bonding with the precursors of SIS, it is critical that the presence of PHFAS does not interfere with the SIS process. Figure 3 shows self-assembly pattern and DSA pattern of VSV/PHFAS after three cycles of SIS [Figs. 3(a) and 3(c)] and after polymer removal by oxygen plasma [Figs. 3(b) and 3(d)]. The clear trenches after polymer removal indicate that no alumina has formed in PS domains, and no wetting layer has formed on top or at bottom of the film. This confirms that the presence of PHFAS does not affect SIS or bring extra complexities to the pattern transfer process compared with pure VSV. Though pitch walking has been observed after polymer removal of the DSA pattern, it mainly comes from the DSA and pattern transfer process rather than the PHFAS, which can be improved by further optimizing the process such as using short PS brush or adjusting the depth of alumina infiltration.<sup>8</sup>

### 3.4 Effect of Molecular Weight of PHFAS on Orientation Control

We have shown that PHFAS can effectively control the orientation of VSV (47k) and achieved DSA line/space pattern with 23-nm full pitch. To apply the same strategy to smaller VSV for sub-10 nm patterning, we investigate the effect of molecular weight of PHFAS on orientation control. We use VSV with three molecular weights (26k, 33k, and 47k) and PHFAS with two molecular weights (5.9k and 9.5k).

The PHFAS dose and annealing conditions were optimized for each VSV. For 26k and 33k VSV, no meaningful results could be observed when mixed with 9.5k PHFAS. This is presumably because the size of PHFAS needs to be similar as or smaller than the P2VP block to interact effectively with the P2VP block, which is further supported by the results when VSV was mixed with smaller PHFAS. When 26k VSV was mixed with 5.9k PHFAS [Fig. 4(a)], similar results were observed as that of 47k VSV mixed with 9.5k PHFAS. Perpendicular orientation began to form as PHFAS dose increased, and full perpendicular lamellae have been achieved with 20% PHFAS at 150°C. For 33k VSV, however, the self-assembled pattern contained many defects after optimization, which could be potentially attributed to the aggregation of PHFAS on top, since PHFAS is also amenable to SIS. Alternatively, the defects could also possibly come from the parallel orientation of VSV with P2VP on top. A more detailed study, such as transmission electron microscopy energy-dispersive X-ray spectroscopy (TEM-EDX), would be helpful to determine the origin of the defects, which could be investigated in the future work. Nevertheless, it has been

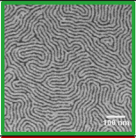
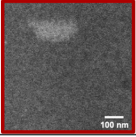
$M_{\text{VSV}}$ (g/mol)	$M_{\text{PHFAS}}$ (g/mol)	$M_{\text{PHFAS}}/M_{\text{VSV}}$	Result
33k	5.9k	0.18	
47k	9.5k	0.20	
26k	5.9k	0.23	
33k	9.5k	0.29	

Fig. 5 Effect of molecular weight of PHFAS on orientation control.

shown that these defects could be eliminated by optimizing molecular weight of PHFAS.

For a more quantitative analysis, we further calculate the ratio of molecular weight of PHFAS ( $M_{\text{PHFAS}}$ ) to the molecular weight of VSV ( $M_{\text{VSV}}$ ) and compare it with the optimized orientation control results, as summarized in Fig. 5. When the ratio is 0.18, after optimizing PHFAS dose and annealing conditions, perpendicular orientation can be observed, however, with defective areas. As the  $M_{\text{PHFAS}}/M_{\text{VSV}}$  ratio increases, orientation control also improves and fully perpendicular lamellae can be achieved. When the ratio is too high, however, no perpendicular orientation can be observed. Consequently, the orientation is best controlled when the ratio is between 0.20 and 0.23, which can provide us a preliminary prediction of the PHFAS size needed for a given VSV.

Among all the combinations, the VSV/PHFAS pair we chose for sub-10 nm patterning is 26k VSV mixed with 20% 5.9k PHFAS [Fig. 6(a)].  $L_0$  is 17.0 nm as measured from FFT analysis. Following the same chemoeptaxy DSA flow, we achieved five times density multiplication on chemical patterns comprising xPS guiding stripes and neutral brush [Fig. 6(b)]. This confirms that our strategy applies to VSV with various molecular weights and periodicities, and therefore could be an effective solution to sub-10 nm patterning.

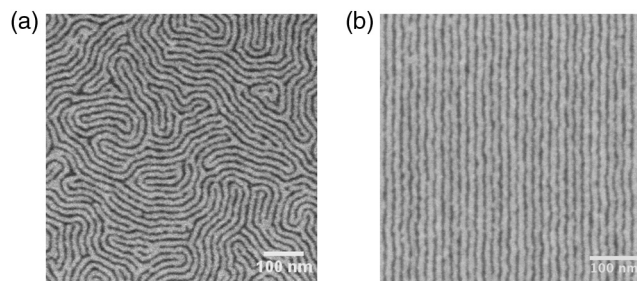


Fig. 6 SEM images of (a) self-assembled VSV on neutral substrate and (b) DSA pattern with 5 $\times$  density multiplication.  $L_0$  is 17.0 nm as measured by FFT analysis.

## 4 Conclusions

In this study, we have demonstrated that PHFAS can effectively balance the surface energies of PS and P2VP blocks, and enable perpendicular orientation of VSV upon simple thermal annealing. After optimizing PHFAS dose and annealing temperatures, we were able to achieve full perpendicular orientation of VSV with  $L_0$  as small as 17 nm. Successful chemoepitaxy DSA with density multiplication was demonstrated, and the pattern transfer potential of this material system has been revealed. We also investigated the relationship between the molecular weight of PHFAS and that of VSV and provided a preliminary prediction of the PHFAS size needed for a given VSV for optimal orientation control. This approach offers an effective solution for sub-10 nm patterning with simple thermal annealing and could be potentially generalized to other high- $\chi$  BCPs as well.

## Acknowledgments

This work was primarily supported by the National Science Foundation (Award No. 1344891). This research used resources at the Center for Nanoscale Materials, a U.S. Department of Energy Office of Science user facility operated by Argonne National Laboratory under Contract no. DE-AC02-06CH11357. The authors are grateful for the support from the NSF Materials Research Science & Engineering Center (MRSEC), Pritzker Nanofabrication Facility, and Searle Cleanroom at the University of Chicago. An earlier version of this work was previously presented at SPIE Advanced Lithography.<sup>19</sup>

## References

1. S. O. Kim et al., "Epitaxial self-assembly of block copolymers on lithographically defined nanopatterned substrates," *Nature* **424**(6947), 411–414 (2003).
2. R. Ruiz et al., "Density multiplication and improved lithography by directed block copolymer assembly," *Science* **321**(5891), 936–939 (2008).
3. R. Gronheid et al., "Defect reduction and defect stability in IMEC's 14 nm half-pitch chemo-epitaxy DSA flow," *Proc. SPIE* **9049**, 904905 (2014).
4. L. Wan et al., "The limits of Lamellae-forming PS- b -PMMA block copolymers for lithography," *ACS Nano* **9**(7), 7506–7514 (2015).
5. X. Gu, I. Gunkel, and T. P. Russell, "Pattern transfer using block copolymers," *Philos. Trans. R. Soc. A Math. Phys. Eng. Sci.* **371**(2000), 20120306 (2013).
6. B. B. Sauer and G. T. Dee, "Surface tension and melt cohesive energy density of polymer melts including high melting and high glass transition polymers," *Macromolecules* **35**(18), 7024–7030 (2002).
7. J. E. Mark, *Physical Properties of Polymers Handbook*, 2nd ed., Springer, New York (2007).
8. S. Xiong et al., "Directed self-assembly of triblock copolymer on chemical patterns for sub-10-nm nanofabrication via solvent annealing," *ACS Nano* **10**(8), 7855–7865 (2016).
9. H. S. Suh et al., "Sub-10-nm patterning via directed self-assembly of block copolymer films with a vapour-phase deposited topcoat," *Nat. Nanotechnol.* **12**(6), 575–581 (2017).
10. J. Zhang et al., "Orientation control in thin films of a high- $\chi$  block copolymer with a surface active embedded neutral layer," *Nano Lett.* **16**(1), 728–735 (2016).
11. A. Vora et al., "Orientation control of block copolymers using surface active, phase-preferential additives," *ACS Appl. Mater. Interfaces* **8**(43), 29808–29817 (2016).
12. S. Ji et al., "Generalization of the use of random copolymers to control the wetting behavior of block copolymer films," *Macromolecules* **41**(23), 9098–9103 (2008).
13. C.-C. Liu et al., "Fabrication of lithographically defined chemically patterned polymer brushes and mats," *Macromolecules* **44**(7), 1876–1885 (2011).
14. P. A. R. Delgadillo et al., "Implementation of a chemo-epitaxy flow for directed self-assembly on 300-mm wafer processing equipment," *J. Micro/Nanolithogr. MEMS MOEMS* **11**(3), 031302 (2012).
15. Z. Sun et al., "Directed self-assembly of poly(2-vinylpyridine)-b-polystyrene-b-poly(2-vinylpyridine) triblock copolymer with sub-15 nm spacing line patterns using a nanoimprinted photoresist template," *Adv. Mater.* **27**(29), 4364–4370 (2015).
16. Y. Matsushita et al., "Molecular weight dependence of lamellar domain spacing of diblock copolymers in bulk," *Macromolecules* **23**(19), 4313–4316 (1990).
17. C. C. Liu et al., "Chemical patterns for directed self-assembly of lamellae-forming block copolymers with density multiplication of features," *Macromolecules* **46**(4), 1415–1424 (2013).
18. Y. C. Tseng et al., "Enhanced block copolymer lithography using sequential infiltration synthesis," *J. Phys. Chem. C* **115**(36), 17725–17729 (2011).
19. J. Li et al., "Directed self-assembly of triblock copolymers for sub-10 nm nanofabrication using polymeric additives," *Proc. SPIE* **10586**, 105860V (2018).

**Jiajing Li** is a PhD candidate in Professor Nealey's group studying directed assembly of functional nanomaterials. She received her bachelor's degree in chemistry from Fudan University in China.

**Paul F. Nealey** is the Brady W. Dougan Professor in the Pritzker School of Molecular Engineering at the University of Chicago. He is a pioneer of directed self-assembly, which is becoming very important in microelectronics processing to create patterns for integrated circuits. He holds numerous honors and has been elected into the National Academy of Engineering for the development of directed self-assembly as an industrially significant process for nanolithography.

Biographies for the other authors are not available.